

# ANALYTICAL INVESTIGATION OF THE GUNN RELAXATION OSCILLATOR OF DOMAIN OPERATING MODES

By

L. ZOMBORY

(Department of Theoretical Electricity, Technical University, Budapest

(Received July 5, 1973)

Presented by Prof. Dr. G. FODOR

## List of symbols

$b$	$= \beta - k$	parameter of the resonant circuit (see (2))
$C$		capacity in the resonant circuit
$h_1, h_2$		parameters of the resonant circuit (see (2))
$k$		ratio of threshold to saturation current
$L$		inductivity in the resonant circuit
$Q$		quality factor of the resonant circuit
$R$		load resistance of the resonant circuit
$R_0$		small signal resistance of the Gunn-diode
$s, s', s_1$		variables of the point transformation
$s_1^*, s_1^{**}$		limits for the fixed point of delayed domain mode
$s_{\max}$		the maximum possible $s$ value in the range of validity of the model (see Fig. 4)
$t$		time
$U_0$		bias voltage of the Gunn-diode
$U_s$		domain sustaining voltage
$U_t$		threshold voltage of the Gunn-diode
$x, y$		state variables (see (1), (2))
$y_1, y_2$		boundary points of the repulsion segment (see Fig. 4)
$y_3$		value of the state variable belonging to the trajectory originating from $s_{\max}$ (see Fig. 4)
$\alpha$		arc ctg $\gamma_2$
$\beta$		ratio of bias to threshold voltage
$\gamma_1, \gamma_2$		normalized damping factor (see (12) and (17))
$\theta_1, \theta_2$		transit angle ( $\theta_i = \Omega_i \tau_i$ )
$\theta_{10}, \theta_{20}$		transit angles belonging to the closed trajectory
$\sigma$		ratio of sustaining to threshold voltage
$\tau$		normalized time ( $\tau = \omega_0 t$ )
$\Psi$		transit angle corresponding to the domain transit time
$\Psi_0, \Psi_2$		defined on p. 265
$\omega_0$		resonant frequency of the resonant circuit
$\Omega_{1,2}$		$\sqrt{1 - h_{1,2}}$
<i>Subscripts</i>		1 state without domain 2 state with domain

## Introduction

Numerous papers are known to discuss the investigation of the sinusoidal operating modes of the Gunn-diode oscillator, using a lumped element model of the diode. Some of them perform numerical investigations only [1–5], others analytical ones [6–16]. But non-sinusoidal (relaxation) oscillations were generally investigated numerically, using either a multi-frequency descrip-

tion function or its modification presupposing a memoryless model [12, 17, 18] or a simple numerical evaluation of a self-consistent description [19–22]. Models relying for their solution on partial differential equations have not been mentioned here.

In this paper a uniform description of the behaviour of the Gunn-diode oscillator operating in domain modes is attempted. The method is applicable for investigating both relaxation and sinusoidal operating modes. In both cases the parameters describing the operation can numerically be determined. These quantities (e.g. the frequency of the oscillation and the amplitude) may be obtained by solving transcendental equations.

In the case of relaxation type oscillations these equations are simpler than the relationships for other methods.

### The investigated model

The lumped element circuit model, basis of the investigation, is seen in Fig. 1. The Gunn-diode is considered as a memoryless element of piecewise linear characteristics with hysteresis (Fig. 2). The  $i_d = u_d/R_0$  section corresponds to the state without domain, while the  $i_d = k \cdot I_t$  section corresponds to the state with domain.

The state equations of the circuit are:

$$C \frac{du_c}{dt} = -i_L - \frac{u_c}{R} - i_d \quad (1a)$$

$$L \frac{di_L}{dt} = u_c \quad (1b)$$

where

$$i_d = \begin{cases} \frac{u_c + U_0}{R_0} & \text{if there is no domain; } R_0 = \frac{U_t}{I_t}, \\ k I_t & \text{if there is a domain.} \end{cases}$$

Introducing the symbols

$$x = R_0 \sqrt{\frac{C}{L}} \frac{u_c}{u_t}; \quad y = \frac{i_L - kI_t}{I_t}; \quad \tau = \frac{t}{\sqrt{LC}} = \omega_0 t,$$

Equ. (1) may be written as:

$$\dot{x} = -2h_{1,2} x - (y + b_{1,2}) \quad (2a)$$

$$\dot{y} = x \quad (2b)$$

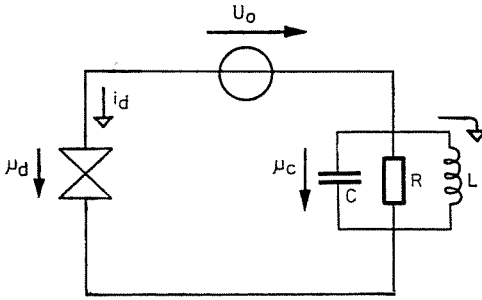


Fig. 1. Model of a Gunn-diode oscillator

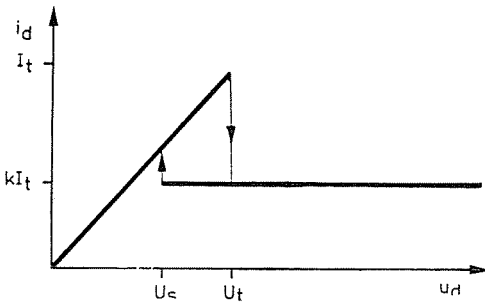


Fig. 2. Characteristics of a Gunn-diode

where

$$h_1 = \frac{1}{2} \left( \frac{1}{R} + \frac{1}{R_0} \right) \sqrt{\frac{L}{C}}; \quad b_1 = \frac{U_0}{U_t} - k = \beta - k = b$$

$$h_2 = \frac{1}{2} \frac{1}{R} \sqrt{\frac{L}{C}}; \quad b_2 = 0.$$

Subscripts 1 and 2 indicate states without, and with domain, respectively.

The conditions of development of the two states are:

– the domain appears when  $u_c + U_0 \geq U_t$ , i.e.

$$x \geq R_0 \sqrt{\frac{C}{L}} (1 - \beta);$$

– the domain disappears when

a) the diode voltage falls below the domain sustaining voltage  $U_s$ :

$u_c + U_0 < U_s$ , i.e.

$$x < R_0 \sqrt{\frac{C}{L}} (\sigma - \beta) \quad \text{where} \quad \sigma = \frac{U_s}{U_t} \quad (k \leq \sigma \leq 1).$$

This case is the *quenched domain* operating mode. The changeover to the state without domain may be considered as a sudden leap.

b) The domain reaches the anode. The diode voltage is supposed to be lower than the threshold voltage  $U_t$  at this moment. This case is the *delayed domain* operating mode. The condition of development will be formulated later using normalized variables.

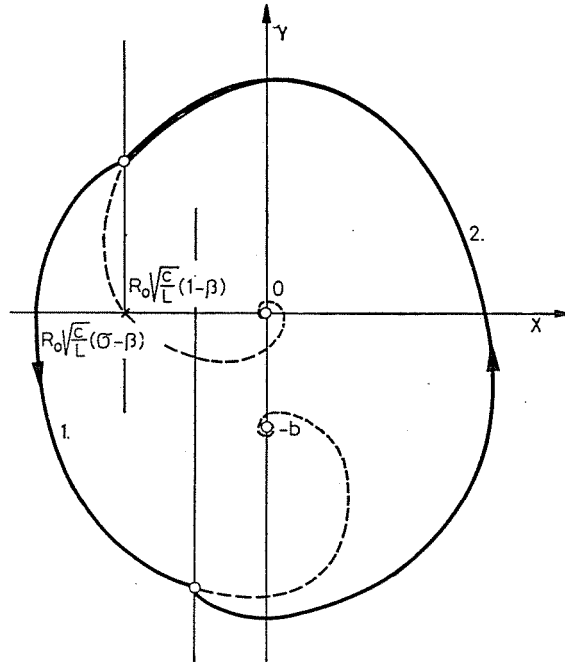


Fig. 3. Closed trajectory of the examined equations on the phase plane

In both modes the periodic operation is conditioned by the existence of a closed trajectory of the describing systems of equations. This trajectory is non-analytic in our case but it consists of two analytic arcs. A closed trajectory is shown in Fig. 3 for quenched domain mode.

### Qualitative behaviours of the describing equations

The only singular points of the system of equations (2) describing the investigated system are  $(0; -b)$  and  $(0; 0)$  in Cases 1 and 2, respectively. In either case it is easy to demonstrate that these singular points are stable. The radius vector belonging to Case 2 is rotated by an angle greater than  $\pi$  as it is seen in Fig. 3.

For  $h_{1,2} > 1$  the singular point is a node. But  $h_2 > 1$  involves  $h_1 > 1$ . If the origin is a stable node in Case 2 then — in view of the above — two

straight trajectories join the node in a sector of central angle  $\pi$ ; no cyclic operation is possible.\*

Consequently, in the following the system of parameters satisfying the conditions  $0 < h_1, 2 < 1$  will only be dealt with.

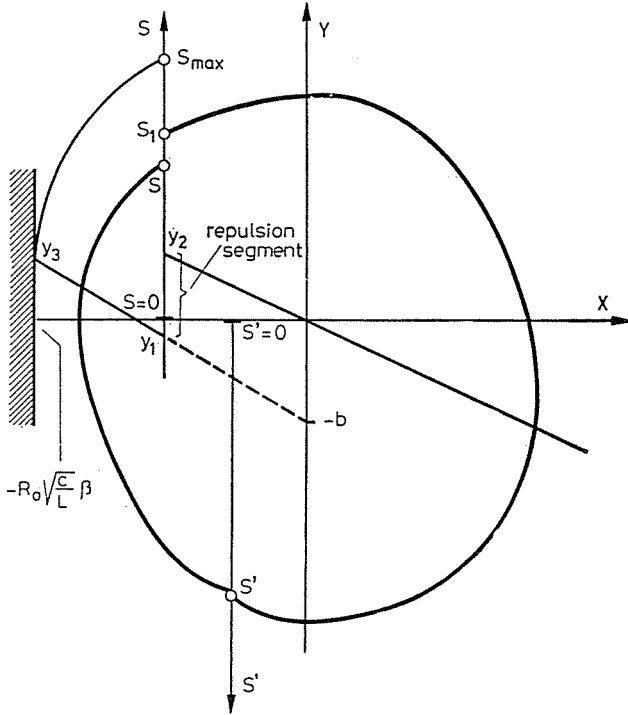


Fig. 4. Phase plane to investigate the point transformation

### Point transformation method for investigating the closed trajectory

Existence and stability of the closed trajectory of the system of equations (2) will be examined by a generalization of Poincaré's successor function method [23, 24, 26]. In Case 1 of the quenched domain mode, the system of equations maps the line  $S$  into the line  $S'$  (point transformation  $\pi_1$ ), while in Case 2 it maps the line  $S'$  into the line  $S$  (point transformation  $\pi_2$ ) (Fig. 4). The natural parameters of the two arcs are time intervals  $\tau_1$  and  $\tau_2$  during which the representative point runs on the arcs. The two successive transformations can be considered as a single transformation  $\pi = \pi_1 \cdot \pi_2$  mapping the line  $S$  into

\* A kind of operation may be realized where the trajectory tending to the node is discontinued because of the finite domain transit time and the nucleation of a new domain begins. Such an operation cannot, however, be described without the consideration of the finite domain dissolution and nucleation time (see e.g. [25]).

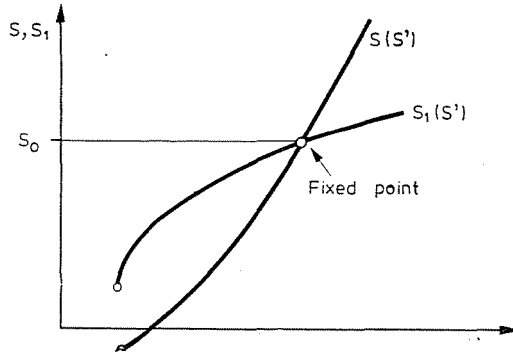


Fig. 5. Lamerey's diagram of the point transformation

itself. If this mapping has a fixed point, the solution of the system of equations has a closed trajectory.

Describing the transformations in the form:

$$\left. \begin{aligned} \pi_1: \quad s' &= \varphi_1(\tau_{10}) & s &= \eta_1(\tau_{10}) \\ \pi_2: \quad s_1 &= \varphi_2(\tau_{20}) & s' &= \eta_2(\tau_{20}) \end{aligned} \right\} \quad (3)$$

the fixed point does exist, if

$$\varphi_1(\tau_{10}) = \eta_2(\tau_{20}) \quad \text{and} \quad \varphi_2(\tau_{20}) = \eta_1(\tau_{10}). \quad (4)$$

The above transcendental equation of two variables  $\tau_{10}$  and  $\tau_{20}$  can be solved numerically. The values of  $s$  and  $s'$  have physical meaning: they are the values of the state variable  $y$  at the moment of the changeover from state 1 to state 2 and vice versa. The values of state variable  $x$  in this moment are fixed.

The problem may be handled graphically, by plotting functions  $s = s(s')$  and  $s_1 = s_1(s')$  of the transformations  $\pi_1$  and  $\pi_2$  in a common coordinate system. (Lamerey's diagram — Fig. 5.) The two curves intersect at the fixed point  $s_0$  of the transformation  $\pi$ . The existence of the fixed point can be deduced from the asymptotic behaviour of the functions.

The closed trajectory is a stable limit cycle if the fixed point is stable. According to Koenig's theorem [23], its condition is the validity of

$$\left| \frac{ds_1}{ds} \right|_{s=s_0} < 1, \quad (5a)$$

while for

$$\left| \frac{ds_1}{ds} \right|_{s=s_0} > 1 \quad (5b)$$

the solution is certainly unstable. Obviously

$$\left| \frac{ds_1}{ds'} \right|_{s=s_1} < \left| \frac{ds}{ds'} \right|_{s=s_1} \tag{6}$$

is a sufficient condition of stability.

In Fig. 5 the fixed point is stable; the corresponding closed trajectory is a stable limit cycle.

The model used above includes two limitations for the trajectories (Fig. 4).

1. The trajectory cannot intersect the S axis at an arbitrarily small value. Let us consider the straight isoclines where

$$\frac{dx}{dy} = \text{const} = \frac{-2hx + (y + b)}{x} \tag{7}$$

The intersections of the isoclines belonging to the vertical tangents and the line S are:

in Case 1:

$$y_1 = -b + \left( 1 + \frac{R_0}{R} \right) (\beta - \sigma) \tag{8}$$

while in Case 2:

$$y_2 = \frac{R_0}{R} \tag{9}$$

at a distance

$$y_2 - y_1 = \sigma - k \geq 0. \tag{10}$$

This part of the line S is the "repulsion segment". Tangents of the trajectory are of opposite direction on either side. Closed trajectory can only exist for  $s_1 \geq y_2$ ; hence  $s > y_1$  according to Eq. (10). This condition will be seen to be fulfilled by the point transformation itself.

2. The trajectory cannot intersect the line S at an arbitrarily high value of s. Namely then the state variable x might attain values of  $x < -R_0 \sqrt{\frac{C}{L}} \beta$ , where the model is not valid any more. Determination of the upper limit of s ( $s_{\max}$  in Fig. 4) will be shown later.

### Quenched domain operating mode

The solution of the system of equations (2):

$$x = e^{-hr} \left( x_0 \cos \Omega \tau - \frac{hx_0 + (y_0 + b)}{\Omega} \sin \Omega \tau \right) \tag{11a}$$

$$y + b = e^{-hr} \left[ (y_0 + b) \cos \Omega \tau + \frac{x_0 + h(y_0 + b)}{\Omega} \sin \Omega \tau \right] \tag{11b}$$

where  $\Omega = \sqrt{1 - h^2}$ , while  $x_0$  and  $y_0$  are the initial values at  $\tau = 0$ .

In transformation  $\pi_1$  at time  $\tau = 0$  the actual values are:

$$x_0 = R_0 \sqrt{\frac{C}{L}} (\sigma - \beta); \quad y_0 = s,$$

while at time  $\tau = \tau_1$

$$x = R_0 \sqrt{\frac{C}{L}} (1 - \beta); \quad y = -s'.$$

The transformation function can be brought arithmetically to the parametric form:

$$s = - \frac{(1 - \beta) e^{\gamma_1 \vartheta_1} - (\sigma - \beta) (\cos \vartheta_1 - \gamma_1 \sin \vartheta_1)}{\frac{1}{R_0} \sqrt{\frac{L}{C}} \frac{1}{\Omega_1} \sin \vartheta_1} - b \quad (12a)$$

$$s' = - \frac{(\sigma - \beta) e^{-\gamma_1 \vartheta_1} - (1 - \beta) (\cos \vartheta_1 + \gamma_1 \sin \vartheta_1)}{\frac{1}{R_0} \sqrt{\frac{L}{C}} \frac{1}{\Omega_1} \sin \vartheta_1} \quad (12b)$$

where

$$\gamma_1 = \frac{h_1}{\Omega_1} = \frac{h_1}{\sqrt{1 - h_1^2}} \quad \text{and} \quad \vartheta_1 = \Omega_1 \tau_1.$$

Only the practically interesting case  $\beta > 1$  will be examined, where  $\beta - \sigma \geq \beta - 1 > 0$  is also valid.

The limits of the normalized time-interval are:  $0 < \vartheta_1 < \pi$  but the lower limit is purely theoretical because if  $\vartheta_1 \rightarrow 0$  then  $s < 0$ , while for a closed limit cycle,  $s > y_2$ .

The transformation function has straight asymptotes:

$$\frac{s + b}{s' - b} \Big|_{\vartheta_1 \rightarrow \pi - 0} = e^{\gamma_1 \pi} (\geq 1) \quad (13a)$$

$$\frac{s + b}{s' - b} \Big|_{\vartheta_1 \rightarrow 0} = -1. \quad (13b)$$

On the basis of the behaviour of the first and second derivatives of function (12) the following properties may be established:

1.  $s'$  has a minimum value where  $s = y_1$ . For parameter values above the pertaining  $\vartheta_1$  the trajectory bypasses the repulsion segment.

2. The curve has an inflection point between the parameter values  $\vartheta_1$  and  $\pi - 0$ , if the condition

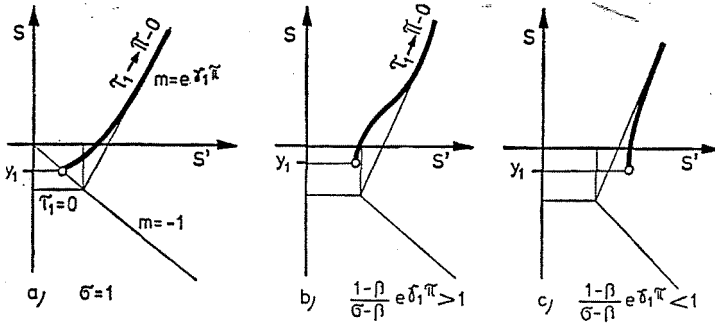


Fig. 6. Function of the point transformation  $\pi_1$

$$\frac{1 - \beta}{\sigma - \beta} e^{\gamma_1 \pi} > 1 \tag{14}$$

is met.

In the limit case  $\sigma = 1$  the curve is convex throughout the domain of the function and for  $\vartheta \rightarrow 0$ ,

$$s = \frac{2(\beta - 1)h_1}{R_0 \sqrt{\frac{L}{C}}} - b \tag{15a}$$

$$s' = b - \frac{2(\beta - 1)h_1}{R_0 \sqrt{\frac{L}{C}}} \tag{15b}$$

All the curves are seen to start from the line  $s + s' = 0$ .

The function sought can be plotted approximately on this basis (Fig. 6).

The lowest possible limit of  $s$  is given by the transformation itself. The upper limit can be assessed as follows: if from the point  $s_{\max}$  on the axis  $S$  to the point of the vertical tangent of the trajectory the parameter varies by  $\vartheta_{cr}$  then, after some arithmetics, we obtain:

$$e^{\gamma_1 \vartheta_{cr}} (\cos \vartheta_{cr} - \gamma_1 \sin \vartheta_{cr}) = \frac{\beta - 1}{\beta} \tag{16}$$

The above equation has one and only one solution in the interval  $[0; \pi]$ .  $s_{\max}$  can be easily calculated if we know  $\vartheta_{cr}$  and  $y_3$ .

The function of the point transformation  $\pi_2$  mapping the line  $S'$  on the line  $S$  is, according to (11):

$$s_1 = \frac{(1 - \beta) e^{-\gamma_2 \vartheta_2} - (\sigma - \beta) (\cos \vartheta_2 + \gamma_2 \sin \vartheta_2)}{R_0 \sqrt{\frac{L}{C}} \frac{1}{\Omega_2} \sin \vartheta_2} \tag{17a}$$

$$s' = \frac{(\sigma - \beta) e^{\gamma_1 \vartheta_2} - (1 - \alpha) (\cos \vartheta_2 - \gamma_2 \sin \vartheta_2)}{\frac{1}{R_0} \sqrt{\frac{L}{C}} \frac{1}{\Omega_2} \sin \vartheta_2} \quad (17b)$$

where

$$\Omega_2 = \sqrt{1 - h_2^2} \quad \text{and} \quad \gamma_2 = \frac{h_2^2}{\Omega_2}.$$

The limits of the transit angle are  $\pi < \vartheta_2 < 2\pi$ , although the upper limit cannot obviously be attained in a periodic operation. The function of transformation (17) has straight asymptotes:

$$\left. \frac{s_1}{s'} \right|_{\vartheta_2 \rightarrow \pi+0} = e^{-\gamma_1 \pi} \quad (18a)$$

$$\left. \frac{s_1}{s'} \right|_{\vartheta_2 \rightarrow 2\pi} = -e^{-\gamma_1 2\pi}. \quad (18b)$$

It may be accepted after having determined the derivatives that the function has a minimum value  $s'$  and the corresponding  $s_1$  is equal to  $y_2$  (Fig. 7).

From (12) and (17) the transit angles  $\vartheta_{10}$  and  $\vartheta_{20}$  can be determined on the basis of (4). The period of oscillation is

$$T = \frac{1}{\omega_0} \left( \frac{\vartheta_{10}}{\Omega_1} + \frac{\vartheta_{20}}{\Omega_2} \right). \quad (19)$$

The qualitative properties of the oscillator can, however, be deduced from the diagram of the transformation functions. In the case shown in Fig. 8 there is a stable limit cycle in the quenched domain mode. [The point of intersection belonging to ordinates lower than the  $y_1$  value (the critical point) is a fictitious one. In the quenched domain mode it has no real limit cycle.]

### Delayed domain operating mode

In the above, the quenching of the domain during the decrease of the diode voltage has been presupposed. If, however, the transit time is less than the time interval belonging to the transit angle  $\vartheta_{20}$  obtained for the stable solution the domain disappears before the voltage drops below  $U_s$ . The domain does not renucleate before the re-establishment of  $U_i$  — this time delay explains the name of the mode.

In Case 2 the transit angle  $\Psi$  is chosen as characteristic ( $\Psi = \omega_0 \Omega_2 t_{\text{transit}}$ ).  $\pi < \Psi < 2\pi$  is obviously valid. Differential equation (2) transforms now the

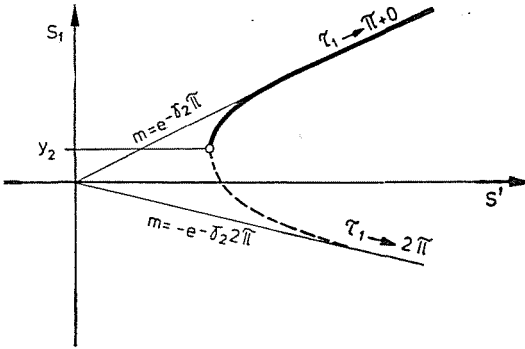


Fig. 7. Function of the point transformation  $\pi_2$

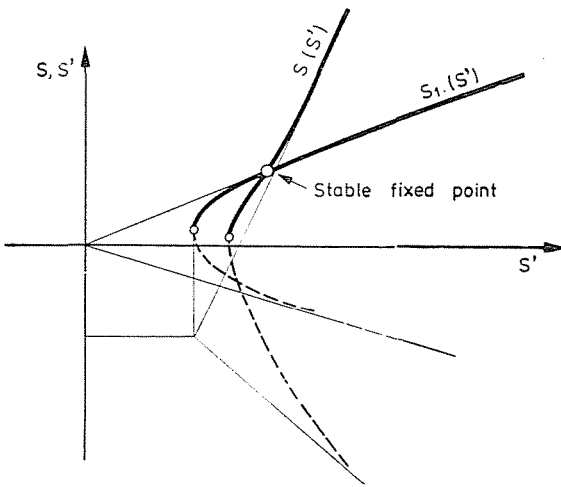


Fig. 8. Lamerey's diagram of the quenched domain mode

line  $S$  into a curve in the phase-plane determined by the parameter  $\Psi$ . From (11) it is evident that this curve is a straight line determined by

$$y = -\frac{\sin(\Psi + \alpha)}{\sin \Psi} x + e^{-\gamma_2 \Psi} R_0 \sqrt{\frac{C}{L}} (1 - \beta) \frac{\sin \alpha}{\sin \Psi} \quad (20)$$

where  $\sin \alpha = \Omega_2$ , hence  $\cos \alpha = h_2$ .

The slope of this line grows beyond limits in the limit cases  $\Psi \rightarrow \pi$  and  $\Psi \rightarrow 2\pi$  (the line is parallel to the  $Y$  axis) while it is zero at  $\Psi_2 = -\alpha$ . In small damping ranges ( $\gamma_2 \approx 0$ )  $\Psi_2 \sim \frac{3\pi}{2}$  and  $\Psi_2$  tends to  $2\pi$  with the growth of the damping.

It is noteworthy that only a part of the straight line contains points leading to any physically real periodical solution in further transformation

(Fig. 9). If the ordinate of the transformed point is higher than  $s_1^*$  then the operation is of quenched domain type; if it is lower than  $s_1^{**}$  then our model cannot describe the processes of domain dissolution — domain nucleation. (For  $\Psi > \Psi_2$ , the above mentioned higher–lower relations will be inverted.) If the operating point coincides with the point  $s_1^{**}$ , the operation is the limit case investigated by Warner [7].  $s_1^*$  and  $s_1^{**}$  can be determined from (17) choosing  $\sigma_1^* = \sigma_{\text{actual}}$  and  $\sigma_1^{**} = 1$ , respectively.

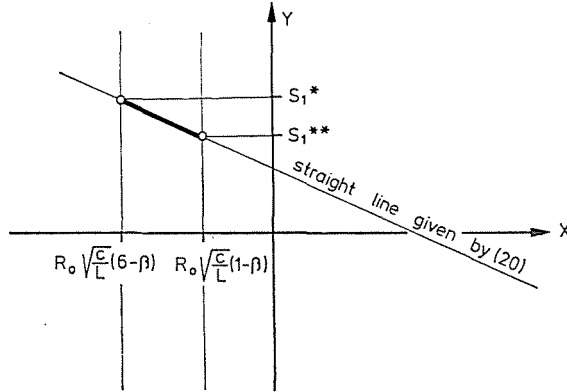


Fig. 9. The allowed points on the phase plane representing the domain dissolution in the delayed domain mode

Of course, all points with ordinates between  $s_1^*$  and  $s_1^{**}$  of the line determined by  $\Psi$  may be re-transformed to the line  $S'$  by transformation  $\pi_1$ . But we performed this transformation only with the value  $\sigma = \sigma_{\text{actual}}$  in the previous (quenched domain) mode, and now  $\sigma$  continuously assumes all values between  $\sigma_{\text{actual}}$  and 1. Both co-ordinates of the transformed point vary linearly together with  $\sigma$ . At the same time it is obvious from (12) and Fig. 6 that for decreasing  $\sigma$  all the points of the function of the transformation  $\pi_1$  are shifted to the right as compared to those for a higher value of  $\sigma$ . Since both  $s$  and  $s'$  vary monotonously with  $\sigma$ , the function of the transformation  $\pi_1$  will be the monotonously varying function shown in Fig. 10 in the delayed domain mode.

At the same time the transformation  $\pi_2$  connecting the  $s'$  value and the ordinates of the transformed points has the following form on the basis of (20):

$$s = - e^{-\gamma_2 \Psi} (\cos \Psi + \gamma_2 \sin \Psi) s' + e^{-\gamma_2 \Psi} \frac{1}{\Omega_2} R_0 \sqrt{\frac{C}{L}} (1 - \beta) \sin \Psi . \quad (21)$$

This function varies together with  $\Psi$  in the way shown in Fig. 11.

A closed trajectory will appear if the curves of the two functions intersect in the range  $s_1^{**} < s < s_1^*$  (or  $s_1^* < s < s_1^{**}$  for  $\Psi > \Psi_2$ ). This trajectory is a stable limit cycle if (6) is met. The diagram of the stable delayed domain mode is shown in Fig. 12.

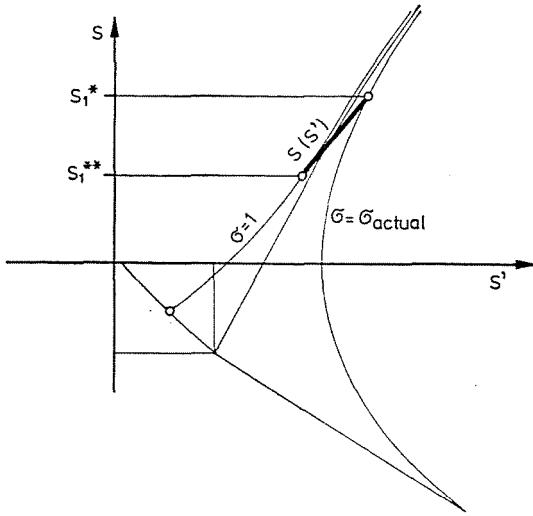


Fig. 10. Point transformation function of the delayed domain mode ( $\tau_1$ )

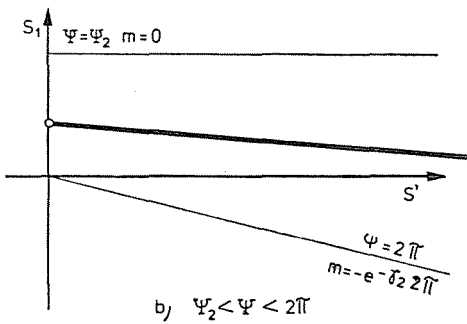
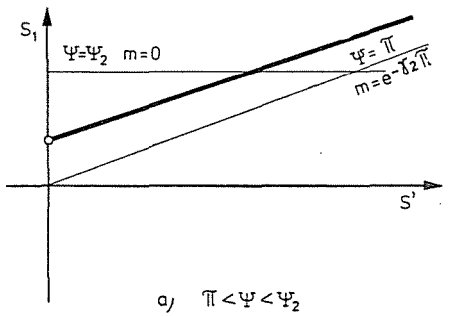


Fig. 11. Point transformation function of the delayed domain mode ( $\tau_2$ )

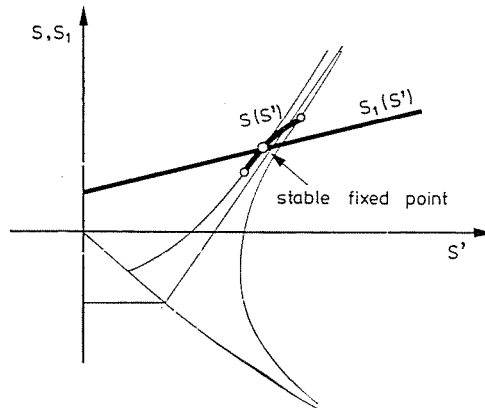


Fig. 12. Lamerey's diagram of the delayed domain mode

To determine the co-ordinates of the fixed point is more difficult here than in the quenched domain mode. Four transcendental equations must be written to obtain the four unknowns  $(s, s', \sigma, \vartheta_{10})$ . The period is

$$T = \frac{\vartheta_{10}}{\omega_0 \Omega_1} + t_{\text{transit}}. \quad (22)$$

### The parameter dependence of the function of point transformations. Tuning

The tuning of the oscillator will be investigated in either operating mode independently. The tuning itself will be represented by changing three parameters:

- i) Bias voltage —  $\beta$
- ii) Resonant frequency —  $\omega_0$
- iii) Load or coupling —  $Q$

By definition

$$Q \triangleq R \sqrt{\frac{C}{L}} \quad (23)$$

consequently, the increase of  $Q$  is equivalent with the decrease of  $1/R$  together with  $h_{1,2}$  and  $\gamma_{1,2}$ .

#### A) Quenched domain mode

i) The  $\beta$  value grows from 1 to an arbitrarily high value. In the case  $\beta = 1$  (it is the case examined by Robson and Mahrous [6] where the diode voltage is purely sinusoidal) the diagram of the transformation  $\Pi_1$  has no

inflection point according to (14). With increasing  $\beta$  the asymptote  $\vartheta_1 \rightarrow \pi - 0$  is shifted to the right, keeping its slope. The  $y_1$  value is the lowest at  $\beta = 1$ ; it may also be negative, if  $R$  has a very large value. With increasing  $\beta$  the  $y_1$  value increases too; if  $\beta \rightarrow \infty$  then  $y \cong \frac{R_0}{R} \beta$ . The diagram of the transformation approaches the limit case  $\sigma = 1$  according to (12) (Fig. 6a). In the case of a sufficiently high  $\beta$ , the critical point  $y_1$  with the minimum value  $s'$  is in the IIInd quadrant of the phase plane.

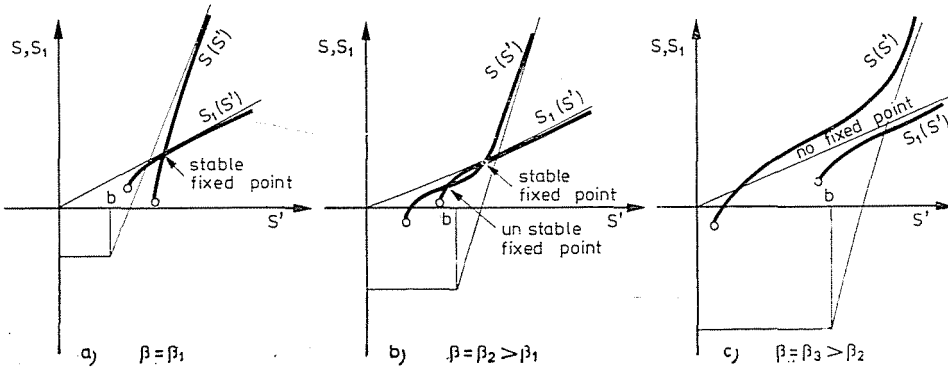


Fig. 13. Variation of the fixed point of the quenched domain mode vs. bias

The asymptotes of the transformation  $\pi_2$  remain unchanged with variable  $\beta$ ; the ordinate  $y_2$  of the critical point grows linearly together with  $\beta$  according to (9). From (17) it is obvious that the critical point is in the ISt quadrant for very high  $\beta$  values. In this case the two curves have no intersection point any more (Fig. 13).

As a conclusion one can obtain a stable limit cycle for low bias voltages; with growing bias an unstable limit cycle appears too; finally the stable limit cycle disappears: the oscillation is discontinued in the quenched mode. This phenomenon is physically due to the more and more disproportionate division of the period among the operating intervals with and without domain.

ii) The variation of  $\omega_0$  does not influence this operating mode because it is not directly included among the parameters. (The real period  $T$  varies of course.) Furthermore it has to be taken into consideration that the model is not valid any more for very high  $\omega_0$  values, since the transition between states 1 and 2 cannot be considered a jump.

iii) With increasing  $Q$  the asymptote  $\vartheta_1 \rightarrow \pi - 0$  of the transformation  $\pi_1$  becomes less sloping, the  $y_1$  value decreases and the curve itself "flares" less and less. At the same time the asymptote  $\vartheta_2 \rightarrow \pi + 0$  of the transformation  $\pi_2$  becomes steeper and steeper with  $y_2$  tending to zero. Thus the point

of intersection of the two asymptotes is continuously shifted towards higher  $s$  and  $s'$  values.

Consequently, the system originally without a stable limit cycle will have one with growing  $Q$  (Fig. 14). The amplitude also grows but this fact does not involve the increase of the output power! Namely with increasing  $Q$ , either the load resistance increases or the coupling becomes weaker.

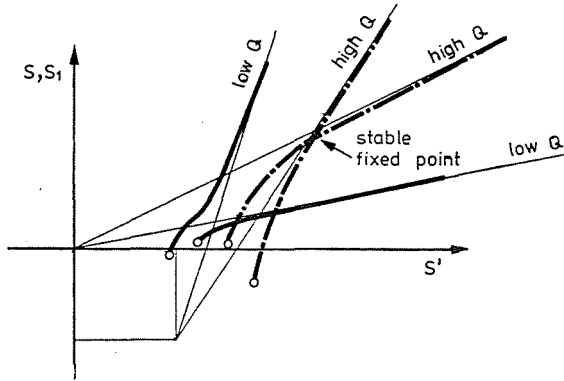


Fig. 14. Variation of the fixed point of the quenched domain mode vs. quality factor

B) Delayed domain operating mode

i) With a constant  $\Psi$  the slope of the transformed image of the line  $s'$  does not depend on  $\beta$ . Consequently  $s_1^*$  and  $s_1^{**}$  are the functions of  $\beta$ , but their difference  $s_1^* - s_1^{**}$  is independent of it. The horizontal distance between the limit points decreases with increasing  $\beta$ , because the curve determined by (12) belonging to the parameter value  $\sigma_{\text{actual}}$  gradually approaches that of parameter  $\sigma = 1$ .

A detailed and very tedious calculation can help to establish three intervals in the allowed domain of the transit angle:  $(\pi, \Psi_2)$ ;  $(\Psi_2, \Psi_0)$  and  $(\Psi_0, 2\pi)$ , having different variation properties with varying  $\beta$ . In the interval  $\pi < \Psi < \Psi_2$  (Fig. 15) with growing  $\beta$  the intersection of the straight line of transformation  $\pi_2$  with the axis and  $s_1^{**}$  vary linearly with  $\beta$ , but the latter grows faster; in the interval  $\Psi_2 < \Psi < \Psi_0$  it grows slower (Fig. 16); while in the interval  $\Psi_0 < \Psi < 2\pi$  the intersection on the axis grows and  $s_1^{**}$  decreases with growing  $\beta$  (Fig. 17). Thus, for any  $\Psi$  there is a bias voltage to which a stable limit cycle belongs. With growing bias voltage this operating mode disappears in each case.

ii) For a fixed transit time  $\omega_0$  and  $\Psi$  are proportional, hence a growing transit angle represents a growing frequency. The change of the limit points

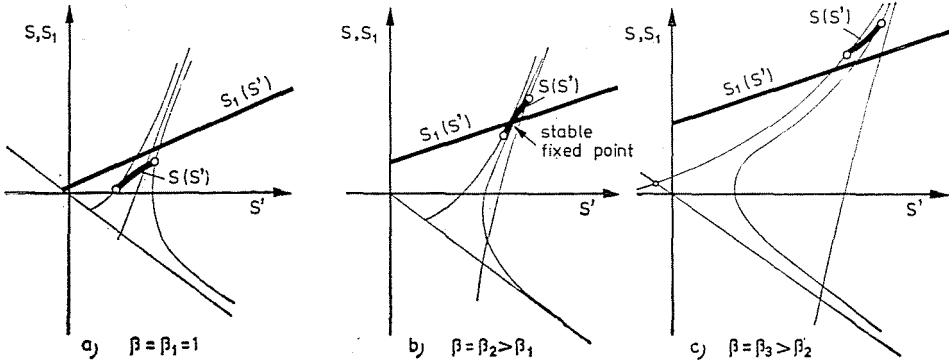


Fig. 15. Fixed point of the delayed domain mode vs. bias ( $\tau < \Psi < \Psi_2$ )

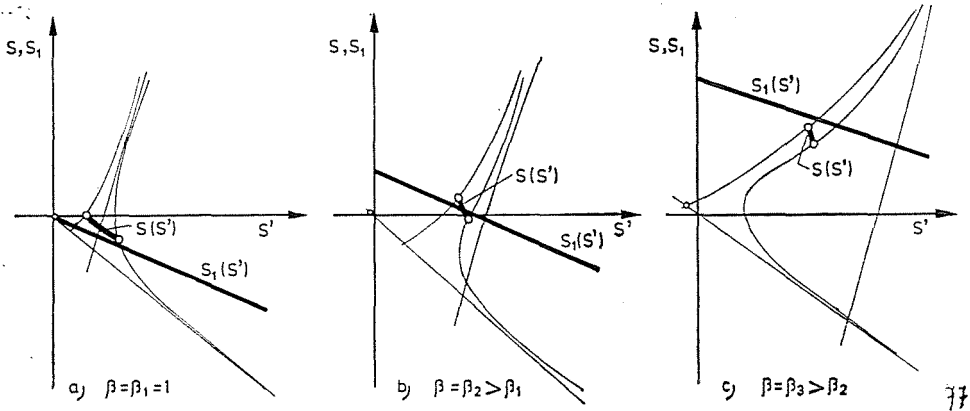


Fig. 16. Fixed point of the delayed domain mode vs. bias ( $\Psi_2 < \Psi < \Psi_0$ )

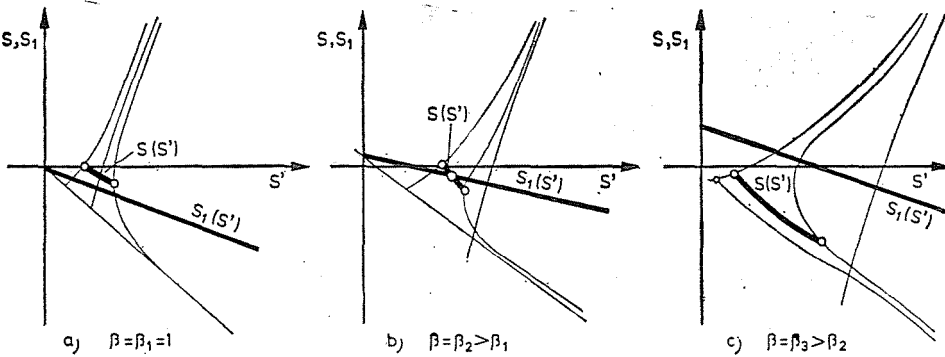


Fig. 17. Fixed point of the delayed domain modes vs. bias ( $\Psi_0 < \Psi < 2\pi$ )

and the arcs between them is shown in Fig. 18. The section bounding the diagram of the transformation  $\pi_2$  is also plotted in the figure.

Comparison of Figs 11 and 18 shows to be no periodic operation for low  $\Psi$  values. With increasing  $\Psi$  (i.e. increasing resonant frequency) a stable fixed point appears. It means with small  $\beta$  (small bias voltage) a stable oscillation with growing amplitude; with higher  $\beta$  a stable oscillation with a first increasing and then decreasing amplitude; while finally, with further increasing the resonant frequency the oscillation ceases.

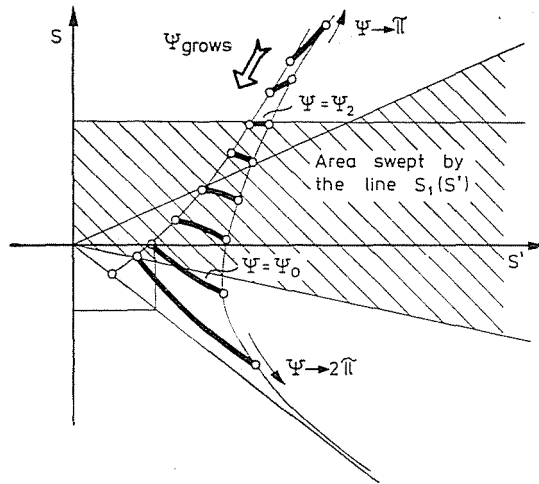


Fig. 18. Variation of the point transformation of the delayed domain mode vs.  $\Psi$

iii) The relations are in rather complicated dependence upon all the parameters. The functions may be discussed in view of the derivatives with respect to  $\gamma_2$ . Two characteristic cases are shown in Fig. 19 for low and high  $Q$  values. Comparison of this figure to Fig. 18 shows that with decreasing frequency the same oscillation mode can develop at a higher  $Q$  value. If the circuit can oscillate at two different  $Q$  values in the same frequency range, then the oscillation can switch over from the mode of low  $Q$  breaking off during the decrease of the frequency to the mode of higher  $Q$  (supposing that the point of intersection of the transformation functions is in the interval  $s_1^* - s_1^{**}$ ). This fact is known from experiments [27], but theoretically has not been explained so far to the knowledge of the author.

### Mode switching in tuning. Hysteresis

In the previous section the tuning properties of the two considered operating modes were investigated separately. The operating mode may, however, change during the process of tuning. These phenomena will be examined in this section.

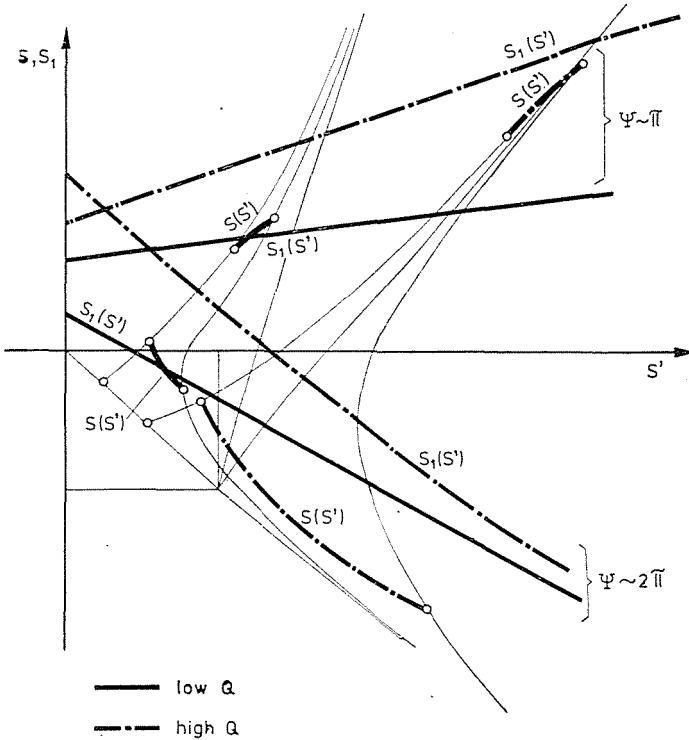


Fig. 19. Variation of the fixed point with increasing  $Q$

A) Varying bias voltage—varying  $\beta$

1.  $\Psi \gtrsim \pi$ .  $s_1^*$  was seen to be of a very high value in general, therefore only the delayed domain mode appears.

2. With increasing  $\Psi$  for  $\beta \cong 1$ , a stable quenched mode appears. With increasing  $\beta$  the stable fixed point attains  $s_1^*$  and the oscillation transits into the delayed domain mode. With further increase of  $\beta$  this mode disappears because the fixed point attains  $s_1^{**}$ .

3. With higher  $\Psi$  the  $s_1^*$  value is so small that the quenched domain mode breaks off (Fig. 14) before the appearance of the delayed domain mode. The possible cases are:

a) The oscillation breaks up finally.

b) If the delayed domain mode has a fixed point, it jumps in (the amplitude decreases) and for a further increase of  $\beta$  the fixed point attains  $s_1^{**}$ . But with decreasing  $\beta$  the delayed domain mode exists as long as the fixed point attains  $s_1^*$ . Only at this moment does the quenched mode step in. The path of the fixed point on the  $s - s'$  plane describes a hysteresis loop. There is no switching on and off at the same values of the parameters.

4. In the case of very high values of ( $\Psi \gtrsim 2\pi$ ) the delayed domain mode appears first and with increasing  $\beta$  it attains the unstable fixed point of the quenched domain mode. In this case the system jumps into the stable quenched mode and the fixed point becomes to move, as outlined in item 3.

It is worth noting that the growth of the quality  $Q$  of the resonant circuit widens the range of the quenched domain mode because the unstable fixed point cannot appear but at very high  $\beta$  values. (See e.g. Fig. 15.)

Remind that the numerical investigations of Tsvirko and Ivanchenko [14] for very high  $Q$  values found the cases 1, 2 and 4 to be the only possible variations for the very reason that they precluded the relaxation types of oscillation.

### B) Varying resonant frequency—varying $\omega_0$

No oscillation for very low  $\omega_0$  (low  $\Psi$  values) is possible at first. With increasing  $\Psi$  the delayed domain mode appears first, later, when the fixed point attains  $s_1^*$  the operation changes over to the quenched domain mode.

There are two other possibilities:  $s_1^*$  coincides either with the unstable or with a fictitious fixed point (curve section over the critical point). The delayed domain mode appears in both cases. With decreasing frequency the inverted process takes place without hysteresis.

If the resonant system (e.g. a resonant cavity) oscillates in several modes and the tuning bands overlap, then the delayed domain mode that became unstable with increasing frequency can be stable again with a cavity mode of lower  $Q$ .

If there is no fixed point of stable quenched domain mode, because the  $\beta$  value is too high, the delayed mode is continuously tuned from the limit point  $s_1^{**}$  to a given value of  $\Psi < 2\pi$ , where the oscillation discontinues.

## Summary

1. A point transformation method has been applied to describe the behaviour of an oscillating system containing Gunn-diode simulated by piecewise linear memoryless characteristics with hysteresis. The method known from the literature has been generalized for the case where the transition between two states of the system occurred at a given moment (delayed domain mode) rather than to be caused by any critical state (quenched domain mode).

2. This method constitutes a simple graphical procedure to examine the tuning of the Gunn oscillator. Variation of the operating modes and their stability as a function of the bias voltage of the diode, the resonant frequency and the quality factor of the oscillating system has been shown. The results are valid both for relaxation type and for nearly sinusoidal oscillations.

3. The conditions of the mode switching and the encountered hysteresis phenomena have been presented, stating a) the possibility of tuning without hysteresis; b) the numerical examination established for harmonic oscillations to be deficient.

4. A partial explanation has been given for an experimentally observed but theoretically unexplained fact, namely how the mode selection in a multimode oscillator and the  $Q$  of each mode are interrelated.

Between limitations of the given simple model rather generalized results have been aimed at. But the involved relationships can be used for the numerical analysis of the oscillators. The calculation requires the solution of transcendental systems of equations.

## References

1. BARBER, M. R.: High power quenched Gunn oscillators. Proc. IEEE **56**, 752—753 (1968).
2. HOBSON, G. S.: The external negative conductance of Gunn-oscillators. Solid-State Electron. **12**, 711—717 (1969).
3. CHEN, W. T.—DALMAN, G. C.: Dynamic  $i-v$  characteristics of a quenched mode oscillating Gunn diode. Proc. IEEE **58**, 503—505 (1970).
4. KHANDELWAL, D. D.—CURTICE, W. R.: A study of the single frequency quenched domain mode Gunn-effect oscillator. IEEE Trans. MTT—**18**, 178—187 (1970).
5. KUZNETSOV, K. V.—LEVINSTEIN, M. E.—SHUR, M. S.: The investigation of the Gunn diode operation in a resonator using the computer model. Solid-State Electron. **14**, 207—220 (1971).
6. ROBSON, P. N.—MAHROUS, S. M.: Some aspects of Gunn-effect oscillators. Radio Electronic Engr. **30**, 345—352 (1965).
7. WARNER, F. L.: Extension of the Gunn-effect theory given by Robson and Mahrous. Electron. Letters **2**, 260—261 (1966).
8. GUNN, J. B.: Effect of domain and circuit properties on oscillations in GaAs. IBM. J. Res. Dev. **10**, 310—320 (1966).
9. HEINLE, W.: Determination of current waveform and efficiency of Gunn diodes. Electron. Letters **3**, 52—54 (1967).
10. CARROLL, J. E.: Mechanisms in Gunn-effect microwave oscillators. Radio Electronic Engr. **34**, 17—30 (1967).
11. LEVINSTEIN, M. E.—SHUR, M. S.: Calculation of the parameters of the microwave Gunn generator. Electron. Letters, **4**, 233—235 (1968).
12. HARRISON, R. I.—DENKER, S. P.—BERGER, H.: A theoretical appraisal of the quenched multiple domain mode in GaAs microwave diodes. Radio Electronic Engr. **37**, 11—15 (1969).
13. TSVIRKO, YU. A. Gunn-effect cavity-controlled generator. Electron. Letters **5**, 107—109 (1969).
14. TSVIRKO, YU. A.—IVANCHENKO, I. A.: Mode tuning and hysteresis behaviour of Gunn-effect cavity controlled generator. Electron. Letters **6**, 9—11 (1970).
15. Андреев, В. С.—Котиков, В. И. Расчет энергетических характеристик генераторов Ганна в режимах с гашением у задержкой домена. Proc. 4th Coll. Microwave Comm. Vol. IV, pp. 3/1—3/10, Akadémiai Kiadó, Budapest, 1970.
16. ALBRECHT, P.: Die Modulation von Gunn-Oszillatoren bei Betrieb im Quenched-Domain-Mode. NTZ. **24**, 516—520 (1971).
17. KINO, G. S.—KURU, I.: High efficiency operation of a Gunn oscillator in the domain mode. IEEE Trans ED—**16**, 735—748 (1969).
18. FREY, W.: Influence of a second harmonic voltage component on the operation of a Gunn oscillator. Proc. MOGA 70 pp. 2/38—2/42, Kluwer-Deventer, The Netherlands, 1970.
19. MANTENA, N. R.—WRIGHT, M. L.: Circuit model simulation of Gunn effect devices. IEEE Trans. MTT—**17**, 363—373 (1969).
20. ROBROCK, R. B. II.: A lumped model for characterizing single and multiple domain propagation in bulk GaAs. IEEE Trans. ED—**17**, 93—102 (1970).
21. GUÉRÉT, P.: Some non-linear properties of a circuit with a Gunn-diode. Proc. MOGA 70, pp. 20/40—20/44, Kluwer-Deventer, The Netherlands, 1970.
22. ZOMBORY, L.—KÓHALMI, Z.—VESZELY, G.: Self-consistent modelling of transferred electron devices. Per. Polytechnica El. Engr. **17**, 27—33 (1973).
23. ANDRONOV, A. A.—VITT, A. A.—KHAIKIN, S. E.: Theory of Oscillators. Pergamon Press, Oxford, 1966.
24. MINORSKY, N.: Nonlinear Oscillations. Van Nostrand, Princeton, 1962.
25. SOLOMON, P. R.—SHAW, M. P.—GRUBIN, H. L.: Analysis of bulk negative differential mobility element in a circuit containing reactive elements. J. Appl. Phys. **43**, 159—172 (1972).
26. Горская, И. С.—Крутова, И. Н.—Рутковский, В. Ю.: Динамика нелинейных сервомеханизмов. Изд. АН СССР, Москва, 1959.
27. TSAI, W. C.—ROSENBAUM, F. J.—MACKENZIE, L. A.: Circuit Analysis of Waveguide-Cavity Gunn-Effect Oscillator. IEEE Trans. MTT—**18**, 808—817 (1970).

Dr. László ZOMBORY, 1502 Budapest, P. O. B. 91, Hungary